

Nanoparticles obtained by confined impinging jet mixer: poly(lactide-co-glycolide) vs. poly--caprolactone

*Original*

Nanoparticles obtained by confined impinging jet mixer: poly(lactide-co-glycolide) vs. poly--caprolactone / Turino, L.N., Stella, B., Dosio, F., Luna, J.A., Barresi, A.A.. - In: DRUG DEVELOPMENT AND INDUSTRIAL PHARMACY. - ISSN 0363-9045. - STAMPA. - 44:6(2018), pp. 934-941. [10.1080/03639045.2017.1421662]

*Availability:*

This version is available at: 11583/2711810 since: 2020-02-22T17:42:32Z

*Publisher:*

TAYLOR & FRANCIS INC

*Published*

DOI:10.1080/03639045.2017.1421662

*Terms of use:*

This article is made available under terms and conditions as specified in the corresponding bibliographic description in the repository

*Publisher copyright*

Taylor and Francis postprint/Author's Accepted Manuscript

This is an Accepted Manuscript of an article published by Taylor & Francis in DRUG DEVELOPMENT AND INDUSTRIAL PHARMACY on 2018, available at <http://www.tandfonline.com/10.1080/03639045.2017.1421662>

(Article begins on next page)

To cite this article:

Ludmila N. Turino, Barbara Stella, Franco Dosio, Julio A. Luna & Antonello A. Barresi (2018) Nanoparticles obtained by confined impinging jet mixer: poly(lactide-co-glycolide) vs. Poly- $\epsilon$ -caprolactone, *Drug Development and Industrial Pharmacy*, **44**:6, 934-941, DOI:10.1080/03639045.2017.1421662

To link to this article: <https://doi.org/10.1080/03639045.2017.1421662>

## **Nanoparticles obtained by Confined Impinging Jet Mixer: Poly(lactide-co-glycolide) vs. Poly- $\epsilon$ -caprolactone**

Ludmila N. Turino<sup>a,b</sup>, Barbara Stella<sup>c</sup>, Franco Dosio<sup>c</sup>, Julio A. Luna<sup>b</sup> and Antonello A. Barresi<sup>a</sup>

<sup>a</sup> *Dipartimento di Scienza Applicata e Tecnologia, Politecnico di Torino, Corso Duca degli Abruzzi 24, 10129 Torino, Italy*

<sup>b</sup> *Laboratorio de Química Fina. Instituto de Desarrollo Tecnológico para la Industria Química (INTEC). Universidad Nacional del Litoral (UNL). Consejo Nacional de Investigaciones Científicas y Técnicas (CONICET). Colectora Ruta Nacional 168, Km 0, Paraje El Pozo, 3000 Santa Fe, Argentina*

<sup>c</sup> *Dipartimento di Scienza e Tecnologia del Farmaco, Università degli Studi di Torino, Via P. Giuria 9, 10125 Torino, Italy*

Corresponding Author: Ludmila N. Turino, E-mail: [lturino@intec.unl.edu.ar](mailto:lturino@intec.unl.edu.ar). Permanent address: Laboratorio de Química Fina. Instituto de Desarrollo Tecnológico para la Industria Química (INTEC). Universidad Nacional del Litoral (UNL). Consejo Nacional de Investigaciones Científicas y Técnicas (CONICET). Colectora Ruta Nacional 168, Km 0, Paraje El Pozo, 3000 Santa Fe, Argentina. Phone: +54 (0)342 4511595. Fax: +54 (0)342 4511079.

**Novelty statement.** Much attention is currently devoted to the development of polymeric nanoparticles by nanoprecipitation method. In this study, for the first time it is reported the comparison between PLGA and PCL polymer nanoparticles produced using a confined impinging jet mixer. Variables like polymer concentration and flow rates are also analyzed. We believe that this approach is particularly innovative and of general interest for the scientific community opening new perspective in nanoparticles synthesis for drug encapsulation technologies.

# **Nanoparticles obtained by Confined Impinging Jet Mixer: Poly(lactide-*co*-glycolide) vs. Poly- $\epsilon$ -caprolactone**

## **Abstract**

This paper is focused on the production and characterization of polymeric nanoparticles obtained by nanoprecipitation. The method consisted of using a confined impinging jet mixer (CIJM), circumventing high-energy equipment. Differences between the use of poly- $\epsilon$ -caprolactone (PCL) and poly(lactide-*co*-glycolide) (PLGA) as concerns particle mean size, zeta potential, and broad spectrum antibiotic florfenicol entrapment were investigated. Other analyzed variables were polymer concentration, solvent and anti-solvent flow rates, and antibiotic initial concentration. To our knowledge, no data were found related to PLGA and PCL nanoparticles comparison using CIJM. Also, florfenicol encapsulation within PCL or PLGA nanoparticles by nanoprecipitation has not been reported yet. The complexity of the nanoprecipitation phenomena has been confirmed, with many relevant variables involved in particles formation. PLGA resulted in smaller and more stable nanoparticles with higher entrapping of florfenicol than PCL.

**Keywords:** Nanoprecipitation, Nanotechnology, Biodegradable polymers, PLGA, PCL, Polymeric drug carriers.

## **1. Introduction**

Nanoparticles are colloidal systems with sub-micron particles size in which drugs can be encapsulated, adsorbed or dispersed. They can be injected directly in the blood stream and the nanoparticle size (for intravenous administration necessarily below 250 nm) reduces the reticulo-endothelial system's interactions, enhancing the circulation time [1]. This is advantageous with respect to other systems such as microparticles, and allows an increased accumulation of the particles (and of the entrapped drug) in tissues with increased vascular permeability and reduced lymphatic drainage such as tumors and inflamed tissues. This phenomenon, named as enhanced permeability and retention effect, is a way of passive targeting of nanoparticles [2-3].

Microparticles and nanoparticles can be obtained with almost the same techniques varying, among many others variables, the energy applied to form the emulsion, the viscosity of the continuous phase, the concentration of surfactants, the phase ratios. In particular, nanoparticles can be prepared by solvent-displacement, a technique also known as nanoprecipitation. By this method a hydrophobic polymer and the drug are dissolved in an organic water-miscible solvent, which is then mixed with an aqueous medium (with or without surfactants or additives). The solvent diffuses in the water phase leading to polymer precipitation and nanoparticle formation. This method is low-energy demanding, easy and fast [4]. It is important to evidence that, even if no surfactants are necessary to obtain nanoparticles by nanoprecipitation [5], they can be useful in some cases.

In the spontaneous process of solid particles formation, the final nanoparticle number and size are determined by rate of mixing, nucleation and self-assembling, growth and aggregation. The nucleation rate depends on polymer structure and solvent phase composition, and can be estimated for example by molecular dynamics [6-8]. The diffusivity rate of the solvent into the non-solvent phase, which depends on the characteristics of the system and is related to the

dielectric constant of the solvent, plays an important role and finally affects the size of the produced nanoparticles [9-12]. The role of the solvent is very complex anyway, as also the type of solvent-water and solvent-water-polymer interactions (that may be enthalpy-controlled or entropy-controlled) since the polymer solubility in the mixture play an important role, as discussed by Ferri et al. [12].

When the solution is added drop by drop to the antisolvent by a syringe, the viscosity of the polymer solution increases affecting the solvent diffusivity; this may be relevant because the regime is mainly laminar and particle formation is governed by Marangoni effect, due to interfacial turbulence [10,13].

A special case of solvent-displacement is achieved with confined impinging jet mixers (CIJM), also known as flash nanoprecipitation, firstly reported by Johnson and Prud'homme [14-15]. By this method, mixing in the center of a cylindrical chamber is extremely rapid due to the impingement of the two opposite streams of organic/polymeric and aqueous phases; attention must be paid anyway to proper selection of the mixer geometry [16-21]. The main advantage of this technology is the possibility to control both the size distribution and the surface properties of the nanoparticles by varying the operating conditions, e.g. polymer concentration, reactor geometry, stream flow rates, quench volumetric ratio, and water-to-organic flow rate ratio, in addition to formulation (polymer and solvent type)[11, 21-25].

Turbulent mixing is important in this type of devices and it allows obtaining smaller particle sizes in comparison to preparation methods where the solution is added drop by drop to the antisolvent; in addition, in case of turbulent precipitation, viscosity has a minor role .

For poly(methoxypolyethylene glycol cyanoacrylate-*co*-hexadecyl cyanoacrylate) (poly(MePEGCA-*co*-HDCA)), PEG-*b*-poly(lactide) and poly- $\epsilon$ -caprolactone (PCL) polymers, literature reported the decrease of nanoparticles mean size with the increment of flow rates for nanoprecipitation processes in intensive mixers [21,25]. In addition, at constant polymer mass

concentration the type of polymer influenced the particle size [26]. All the previously cited articles studied the effect of the relevant variables using different types of polymers for nanoparticles preparation and entrapment of different hydrophobic drugs, but information related to poly(lactide-*co*-glycolide) (PLGA) nanoparticles preparation using CIJM has not been reported yet. As a way to comparison, we propose the study of PLGA and the well characterized PCL for nanoparticles preparation, both representative of an important group of synthetic aliphatic polyesters preferably used as polymeric matrix in pharmaceutical formulations because of their approval by the FDA. PCL and PLGA (Fig. 1) are commonly used in the design of controlled release formulations due to their biodegradability (by bulk hydrolysis of the ester bonds) and biocompatibility properties [27]. PLGA formulations are very versatile: molecular weight, ratio of polylactide to polyglycolide, end-group of polymeric chains can be modified and adjusted to meet required release patterns of a dosage form [28]. PCL, on the other hand, is interesting for its slower degradation, its low cost and its ability to form blends with other polymers [1,29].

Florfenicol (2,2-dichloro-*N*-[(1*R*,2*S*)-3-fluoro-1-hydroxy-1-(4-methanesulfonylphenyl)propan-2-yl]acetamide) (Fig. 1) is a broad-spectrum antibiotic, active (bacteriostatic) against many gram-negative and gram-positive organisms. Florfenicol molecule has a fluorine atom in its structure making it more resistant to deactivation by bacteria than chloramphenicol. Florfenicol commercial formulations are indicated in the treatment of respiratory infections and pododermatitis in cattle [30]. Few studies are available on the synthesis of nanocarriers containing this drug: Song et al. [31] obtained silica nanoparticles with adsorbed florfenicol; Kou et al. [32] studied its adsorption on molecularly imprinted nanospheres obtained by premix membrane emulsification method; Pinto et al. [33] prepared florfenicol-PLGA nanoparticles using an emulsion/diffusion/evaporation method; while Wang et al. [34] prepared florfenicol-loaded solid lipid nanoparticles by hot

homogenization and ultrasonic technique. To our knowledge, florfenicol encapsulation within PCL or PLGA nanoparticles using nanoprecipitation in CIJM has not been reported yet. The feature of being slightly soluble (and not insoluble) in water makes its loading into hydrophobic polymeric matrices challenging.

In the present contribution, authors studied the influence of the polymer (PCL or PLGA) characteristics over particles size and florfenicol entrapment using the solvent displacement method in a CIJM which, as discussed, is a technique that allows reproducible and controlled production of nanocarriers for controlled release.

## **2. Materials and Methods**

### ***2.1 Materials***

Commercially available uncapped low molecular weight 50:50 PLGA Resomer<sup>®</sup> RG502H ( $M_w$  8650 Da, Boehringer Ingelheim Pharma KG, Germany), PCL ( $M_w$  14000 Da, Sigma-Aldrich, Germany), florfenicol (99.2%, Chemo Romikin, Argentina), acetone (Sigma-Aldrich, Germany) were used for nanoparticles preparation. Ultrapure water was used as non-solvent phase (Milli-Q RG, Millipore System, Germany).

### ***2.2 Nanoparticles Preparation***

The nanoprecipitation method was implemented, using a CIJM for the precipitation of the polymer. Acetone has been selected as polymer solvent for its high diffusivity in water, which allows to obtain smaller particles than other solvents (like dimethylformamide, acetonitrile or tetrahydrofuran) without the undesired upsizing phenomenon at high Reynolds number [11].

The used CIJM consisted of a T-type mixer with an internal mixing chamber, two opposite inlet tubes, and one outlet tube (Fig. 2). The CIJM was used as a passive mixer where the polymer-containing acetone solution (eventually containing also the drug) and water streams were fed into the chamber by a syringe pump (KDS200; KD Scientific, USA) and mixed

under turbulent flow conditions thanks to the kinetics energy of the impinging jets. Equal water and solvent flow rates were considered in this work. In order to kinetically freeze the produced nanoparticles and stabilize the particle suspension, the outlet stream was collected into water and kept gently stirred. A quench ratio of 1:1 (ratio between quantity of water used in CIJM and water in the collecting bath) was used, as this value is an optimal compromise between size control and suspension dilution [25]. Acetone was evaporated from suspension in a rotary evaporator (Stuart Rotary Evaporators, Bibby Scientific Ltd., UK) for 30 min.

In a first instance, three different flow rates and three initial polymer concentrations in acetone were evaluated for blank nanoparticles preparation using PCL and PLGA polymers. After the characterization of these nanoparticles, variable drug initial concentrations were included in the polymer containing phase (at fixed polymer concentration of 6 mg/mL) and different flow rates were investigated to evaluate the effect on particle mean size and surface zeta potential. The encapsulation of florfenicol was evaluated in nanoparticles obtained under the following conditions: polymer concentration 6 mg/mL and flow rate 80 mL/min. In Table 1 operating parameters are summarized for all the prepared particles. After acetone evaporation, nanoparticles suspensions were stored at 4°C for further analysis. Assays were conducted in triplicate to study the reproducibility of the methodology.

## ***2.3 Nanoparticles Characterization***

### ***2.3.1 Mean Size and Zeta Potential***

First, each suspension was diluted properly with ultrapure water. Then, the size distribution was analyzed by dynamic light scattering (Zetasizer Nanoseries ZS90, Malvern Instrument). The mean size value from the intensity distribution (called the *Z* average) and the polydispersity index (PDI), to describe the size distribution width, were considered. Electrophoretic measurements were also carried out in the same equipment to measure the zeta potential of the nanoparticles. Data were analyzed using statistical tools (ANOVA and

Fisher LSD tests). The differences between experiments were considered significant when  $p < 0.05$ .

### 2.3.2 Drug Incorporation

The drug encapsulation efficiency and the drug loading were estimated with an indirect method, consisting in the centrifugation of a fixed volume of suspension, containing a known mass of nanoparticles ( $M_{np}$ ) (45,000 rpm for 90 min; Ultracentrifuge L5-50B, TY65 rotor type, Beckmann) and determining the unloaded mass of drug ( $M_{uld}$ ) in the supernatant. Concentration of florfenicol was measured spectrophotometrically at 223 nm (Beckman Du-700), using a previously obtained calibration curve in water ( $R^2 = 0.999$ ).

The loaded mass of antibiotic could be calculated as difference between the initial mass of florfenicol used during nanoparticles preparation ( $M_i$ ) and  $M_{uld}$ . As a result, the quantity of entrapped drug (drug loading,  $En$ ) was estimated based on Eq. (1):

$$\%En = \frac{(M_i - M_{uld})}{M_{np}} 100 \quad (1)$$

in which  $En$  is grams of entrapped florfenicol in 100 g of nanoparticles (% w/w). Eq. (2) was used to calculate the encapsulation efficiency ( $Ee$ ):

$$\%Ee = \frac{(M_i - M_{uld})}{M_i} 100 \quad (2)$$

## 3. Results and Discussion

The mean size of nanoparticles obtained at different flow rates and at three polymer concentrations of PCL and PLGA is shown in Figure 3a. Results are presented as mean values and standard deviations of three independent assays. The 94% of variations between repetitions of the same assay resulted in deviations lower than 9.1% on the mean particle size, demonstrating high reproducibility of nanoparticles preparation method.

It is generally accepted that an increase in the flow rates of the two opposite streams will produce a higher number of smaller particles, because the improved mixing performance favors the formation of higher supersaturation levels and thus higher nucleation rates. Equivalently, if formation by self-assembly is assumed, the particle size is proportional to the ratio of the mixing and coalescence, but the process can still be approximated by the expression used for homogeneous nucleation. The size-flow rate-concentration relationships can be described by the following power law:

$$d_p = Av_j^\beta c_{\text{pol}}^\alpha \quad (3)$$

where  $d_p$  is the mean nanoparticle size,  $A$  is a coefficient that depends on polymer and also on the geometry of the mixer,  $v_j$  is the inlet fluid velocity, both  $\alpha$  and  $\beta$  are parameters from power law equation (where  $\alpha=0.29$  and  $\beta=-0.18$  for both polymers [25]), and  $c_{\text{pol}}$  is the initial polymer concentration. From present data, the dependence of particle size on  $v_j$  (variable which is proportional to the volumetric feed flow rate) does not appear to be very strong. Anyway, it must be considered that the particle volume is proportional to the cube of the diameter, and considering this variable, its dependence on inlet velocity is more significant. The effect is generally evident particularly at flow rates lower than the investigated range, where the flow is not completely turbulent. In addition, when the mixing time becomes comparable with the characteristic particle formation time, the increase of the mixing efficiency, obtained increasing the feed rate and thus the turbulence intensity, increases productivity but has no beneficial effect on the particle size. The break point occurs in this case at flow rate in the range 50-80 mL/min. On the contrary, the increase of turbulence level is responsible for higher pressure drops and can favor aggregation phenomena; it must be remembered anyway that for particles lower than micron size Brownian (perikinetic) aggregation is more important than orthokinetic one [35].

The curves shown in Figure 3a are those predicted with the power law relationship given in Eq. (3). The obtained results are in agreement (considering experimental uncertainty) with previous results obtained with the same device for PCL, confirming the dependence of particle size on  $v_j^{-0.18}$ . Figure 3a also evidences a similar dependence for PLGA.

The differences between the two polymers could be attributed to differences in the respective characteristic particle formation time. Literature results have shown that the particle size dependence on inlet fluid velocity can change in a very limited range for different polymers. On the other hand, the size of the obtained particles can be largely different, as in the present case, because it depends on polymer structure and also on molecular weight [26]. These previously published results showed that larger PCL particles than poly(MePEGCA-co-HDCA) or the homopolymer PHDCA ones were obtained, and in the case of PCL larger particles were obtained when a polymer with higher molecular weight was used, both at equal initial polymer concentration. As a consequence, for a given initial polymer concentration, also the number of particles formed is very different, which can be easily estimated considering that the precipitation is very fast and yield is generally close to unit [22]. In the investigated range PLGA nanoparticles have a diameter that is about one third of the PCL ones, but their number is 20-40 times larger in the different operating conditions.

As discussed, the role of viscosity is generally marginal for solvent displacement in this turbulent regime, differently from what has been proposed using different techniques, like the emulsion polymerization, where the size of the formed droplets may be affected by the polymer solution viscosity [36-38].

The effect of polymer concentration on mean particle size is evidenced in Figure 3b. The increase observed for both PCL and PLGA is in agreement with previous findings for various polymers and can be described by the same power law type relationship (see Eq. (3)), indicating that, in this relatively low concentration range, particle formation can be interpreted

by a nucleation-aggregation mechanism that is typical of high supersaturation conditions [26,39]. Exponent values reported in literature for different polymers vary in a wider range than for the flow rate dependence, but for PCL and PLGA the data obtained in this work suggest the same dependence (that is size proportional to  $c_{\text{pol}}^{0.29}$ ).

A further difference in the behavior of PCL and PLGA can be evidenced looking closer at the relative size variation of the particles. In fact, if the size-flow rate-concentration relationships were perfectly described by the power laws previously proposed in Eq. (3) (and showed in Figure 3a and 3b), the relative size variation of the particles should be the same at any flow rate. Figure 4a shows the values of the relative size increments (that is the size variation with respect to the case with the lowest polymer concentration tested, 2.5 mg/mL, at the same flow rate). Even if the data must be analyzed with caution, because small differences may be strongly affected by experimental uncertainty, the different trend is evident. The quantitative justification is difficult due to the complexity of the phenomena involved, but the increase observed at higher flow rate for PCL can be explained with size increase due to aggregation. PCL nanoparticles are less stable than PLGA nanoparticles (as shown by the comparison of the respective zeta potential values), and growth by particle aggregation may be more relevant.

More difficult is the explanation of the PLGA behavior, which is probably related to the role of nucleation, which is more important for this polymer as demonstrated by the smaller average size and is influenced by polymer concentration in a strongly non-linear way. Estimating the number of particles formed, in fact, it can be noted that the smaller size increase for PLGA corresponds to a stronger increase in particle number.

The variation of the polydispersity is shown in Figure 4b; the graph describes the dependence of the distribution width on the inlet polymer concentration. The efficacy of nanoparticle formulations is based on their nano-size and low polydispersity, ensuring injectability,

reproducibility, appropriate circulating time in blood, and release performance. It is worth to note that, independently of the type and concentration of polymer and flow rates, all nanoparticles suspensions had a PDI lower than 0.20 and can be considered monodispersed distributions [40]. Besides the fact that PCL nanoparticles reach greater mean size values, their PDI was significantly lower than PLGA and below 0.10. This confirms the complexity of the nanoprecipitation phenomenon, where many variables (more than those analyzed in the present contribution) are involved during particles formation. Since acetone is miscible with water, there is no emulsification step and nanoparticles formation starts immediately [41]. Under the same operating conditions, differences in polymer solubility in both solvent and non-solvent would determine variations between PCL and PLGA precipitation conditions (supersaturation, self-assembling rate, Ostwald ripening) and thus on the final particle size distribution properties [42]. Moreover, Bilati et al. [10] found that a more hydrophobic polymer produced larger particles by nanoprecipitation using the syringe method. In the present contribution, this empirical rule seems confirmed as the more hydrophobic PCL (semi-crystalline polymer) compared with PLGA (amorphous polymer) [27,29] forms bigger nanoparticles (about 300 nm against 100 nm) (Fig.1 and 3a).

Zeta potential values of all studied nanoparticles are presented in Figure 5a. All nanoparticles resulted negatively charged due to the presence of ionized carboxylate end-groups from PCL and PLGA polymeric chains on particle surface [4,43]. The particle surface charge is a factor that determines the physical stability of nanoparticles. The higher is the absolute zeta potential value, the more stable is the nanoparticles suspension; in fact, when particles are largely and equally charged, the electrostatic repulsion forces between the particles are higher and agglomeration diminishes [44]. For both analyzed polymers the particle stability was higher for the larger particles, produced starting from higher initial polymer concentrations; no significant influence of flow rate was evidenced.

Comparing the results obtained for the two different polymers, it can be noted that PLGA nanoparticles reach zeta potential values between  $-32$  and  $-40$  mV while PCL values were above  $-25$  mV. In scientific and industrial fields, the common dividing line between unstable and stable suspensions is taken as  $+30$  or  $-30$  mV: therefore PLGA formulation can be considered as physically stable while PCL suspensions have a lower stability [45]. Despite this, all the PCL suspensions prepared from different initial concentration of polymer maintained the initial properties with respect to mean size after three months of storage at  $4^{\circ}\text{C}$  ( $p > 0.05$ ) (data not shown). In Figure 5b it can be seen a linear regression analysis between zeta potential and mean size values of all prepared nanoparticles. Especially in case of PCL, the inverse proportionality is clearly evident ( $R = 0.922$ ), at least in the investigated range. It is well known that reducing the size distribution of dispersion, stability is increased because sedimentation or cremation effects are reduced [38]. In this case, the effect is counteracted by the zeta potential variation, because for smaller sizes the absolute zeta values decrease.

Florfenicol was incorporated during nanoparticles preparation in the acetone phase at four concentration levels between  $0.5$  and  $5$  mg/mL (see Table 1 for additional information on operating parameters). Mean size and zeta potential of nanoparticles prepared from  $6$  mg/mL PCL and PLGA solutions at three flow rates are shown in Table 2 and Table 3, respectively. In most cases, nanoparticles did not significantly change their size when the concentration of florfenicol increased. Similar results were reported by Corrigan and Li [46] after the entrapment of indomethacin and ketoprofen inside PLGA RG504 nanoparticles by single emulsion technique. It is important to mention anyway that in literature generally the size increases with loading [26,47].

To confirm the drug entrapment,  $En$  was evaluated for nanoparticles prepared at a flow rate of  $80$  mL/min. Results for PCL and PLGA nanoparticles are shown in Table 4. Entrapped quantities of antibiotic increased when greater initial amounts of florfenicol were used during

nanoparticles preparation. Similar results were reported by other authors for different solvent-polymer-drug systems using the nanoprecipitation method [5,9,47-48]. Pinto et al. [33] also increased florfenicol encapsulation efficiencies into PLGA nanoparticles by emulsion/diffusion/evaporation method and varying the initial mass of drug. Taking into account the polymer type, PCL leads to nanoparticles with significant levels of loaded florfenicol only at antibiotic initial concentrations higher than 2 mg/mL. At initial florfenicol concentration of 0.5 and 1 mg/mL no drug entrapment could be detected. Despite this, a notable increment in  $En$  was achieved at 5 mg/mL florfenicol concentration, reaching values around 10% w/w. For PLGA nanoparticles, the increment was more gradual, with  $En$  values varying from 0.76 to almost 13% w/w for the four initial antibiotic concentrations. It is worth to note that PLGA nanoparticles with a mean size around 95 nm entrapped almost four times more florfenicol than PCL nanoparticles (260 nm) when initial 2 mg/mL of antibiotic was used (Tables 2-4). This different behavior could be related to physico-chemical differences between obtained polymeric matrixes and to different mechanisms of incorporation that can be connected to differences in hydrophobicity of the polymer/solvent system. In other words, factors related with core hydrophobicity, polymeric molecules self-assembly, internal pore distribution, and surface properties could be responsible for drug entrapment differences between PCL and PLGA, especially if the same operating conditions (flow rate, CIJM geometry) and formulation parameters (solvent type, polymer concentration, drug concentration) were used. In the same way, different polymer-drug interactions may play an important role with regards to drug loading: Barichello et al. [49] discussed about this phenomenon by analyzing the incorporation of hydrophilic and lipophilic drugs into PLGA particles by nanoprecipitation. If the solubility of florfenicol in water is considered (the drug is slightly soluble), the above mentioned more hydrophobic nature of PCL would be

associated with a lower entrapment than PLGA due to the lower affinity of hydrophilic drugs for hydrophobic polymers.

Florfenicol-PCL particles had zeta potential absolute values lower than 30 mV and were still considered with a limited stability (Table 2). Nanoparticles obtained using 6 mg/mL of PLGA at different concentrations of florfenicol were stable (Table 3). Moreover, the lack of differences between zeta potential with and without adding florfenicol into formulation could suggest the absence of adsorbed antibiotic on the surface of nanoparticles. In other words, data suggest that all the nanoparticle-associated drug is inside polymeric matrix.

Besides the fact that drug loading between 10 and 13% w/w for PCL and PLGA matrices, respectively, was obtained, encapsulation efficiencies were low (around 15%), leaving high wasted quantities of antibiotic out of nanoparticles when such a high quantity of drug was added during nanoparticle preparation. Since nanoprecipitation is most suited for hydrophobic drugs, the poor efficiencies could be also related with the considerable solubility of florfenicol in water at room temperature (around 1000 ppm [31]). This promotes more drug partition in water-solvent mixture during nanoparticles preparation due to relatively high residual solubility in the mixture [46,50]. Despite this, Alshamsan [41] compared nanoprecipitation against solvent evaporation method for the encapsulation of a polar molecule and found that the first reached a drug loading 12 times higher. Polymer concentrations could be increased in order to favor encapsulation but at risk of size distribution increase, as discussed above.

Moreover, in literature Misra et al. [43] emphasizes the use of polymeric blends (PLGA:PCL) to favor entrapment of hydrophilic drugs by solvent evaporation technique. Bilati et al. [10] proposes the use of alcohols as non-solvents to prevent drug partition into aqueous medium and Govender et al. [9] analyzed other formulation approaches for improving hydrophilic drug encapsulation efficiencies by nanoprecipitation.

#### **4. Conclusions**

CIJM devices resulted especially attractive for nanoparticles production in a reproducible way. In this work in particular we have compared PCL and PLGA matrices concerning their ability to produce nanoparticles and entrap florfenicol. Differences in mean size, PDI and zeta potential could be found between nanoparticle formulations obtained from different polymer types, polymer concentrations, and flow rates; this resulted in smaller and more stable nanoparticles suspensions for PLGA than PCL. After florfenicol incorporation at four concentrations, PCL and PLGA nanoparticles did not change their mean size or surface zeta potential. Entrapment was increased for higher initial concentrations of drug. PLGA matrix was more able to entrap this slightly hydrophilic antibiotic with respect to PCL due to its less hydrophobic nature.

**Acknowledgments:** This work was supported by Politecnico di Torino, MIUR, University of Turin “Fondi Ricerca Locale (ex-60%)”, Consejo Nacional de Investigaciones Científicas y Técnicas (CONICET), and Universidad Nacional del Litoral (UNL) of Argentina.

**Conflict of Interest:** The authors declare that they have no conflict of interest.

#### **References**

[1] Sinha VR, Bansal K, Kaushik R, et al. Poly- $\epsilon$ -caprolactone microspheres and nanospheres: an overview. *Int J Pharm.* 2004;278:1-23.

[2] Cho K, Wang X, Nie S, et al. Therapeutic nanoparticles for drug delivery in cancer. *Clin Cancer Res.* 2008;14:1310-6.

[3] Shaji J, Lal M. Nanocarriers for targeting in inflammation. *Asian J Pharm Clin Res.* 2013;6:3-12.

[4] Singh Y, Ojha P, Srivastava M, et al. Reinvestigating nanoprecipitation via Box-Behnken design: a systematic approach. *J Microencapsul.* 2015;32:75-85.

[5] Le Roy Boehm A-L, Zerrouk R, Fessi H. Poly- $\epsilon$ -caprolactone nanoparticles containing a poorly soluble pesticide: formulation and stability study. *J Microencapsul.* 2000;17:195-205.

[6] Di Pasquale N, Marchisio DL, Carbone P, et al. Identification of nucleation rate parameters with MD and validation of the CFD model for polymer particle precipitation. *Chem Eng Res Des.* 2013;91:2275-90.

[7] Di Pasquale N, Marchisio DL, Barresi AA, et al. Solvent structuring and its effect on the polymer structure and processability: The case of water–acetone poly- $\epsilon$ -caprolactone mixtures. *J Phys Chem B.* 2014;118:13258–67.

[8] Lavino AD, Di Pasquale N, Carbone P, et al. A novel multiscale model for the simulation of polymer flash nano-precipitation. *Chem Eng Sci.* 2017;171:485-94.

[9] Govender T, Stolnik S, Garnett MC, et al. PLGA nanoparticles prepared by nanoprecipitation: drug loading and release studies of a water soluble drug. *J Control Release.* 1999;57:171–85.

[10] Bilati U, Allémann E, Doelker E. Development of a nanoprecipitation method intended for the entrapment of hydrophilic drugs into nanoparticles. *Eur J Pharm Sci.* 2005;24:67–75.

[11] Chow SF, Sun CC, Chow AHL. Assessment of the relative performance of a confined impinging jets mixer and a multi-inlet vortex mixer for curcumin nanoparticle production. *Eur J Pharm Biopharm.* 2014;88:462–71.

[12] Ferri A, Kumari N, Peila R, et al. Production of menthol-loaded polymeric nanoparticles by solvent displacement. *Canad J Chem Eng.* 2017;95(9):1690–706.

- [13] Sonam, Chaudhary H, Kumar V. Taguchi design optimization and development of antibacterial drug-loaded PLGA nanoparticles. *Int J Biol Macromol.* 2014;64:99-105.
- [14] Johnson BK, Prud-homme RK. Flash nanoprecipitation of organic actives and block copolymers using a confined impinging jets mixer. *Aust J Chem.* 2003;56:1021-24.
- [15] Johnson BK, Prud-homme RK. Mechanism for rapid self-assembly of block copolymer nanoparticles. *Phys Rev Lett.* 2003;91:1183021-4.
- [16] Johnson BK, Prud-homme RK. Chemical processing and micromixing in confined impinging jets. *AIChE J.* 2003;49:2264-82.
- [17] Lince F, Marchisio DL, Barresi AA. Strategies to control the particle size distribution of poly- $\epsilon$ -caprolactone nanoparticles for pharmaceutical applications. *J Colloid Interf Sci.* 2008;322:505-15.
- [18] Lince F, Marchisio DL, Barresi AA. Smart mixers and reactors for the production of pharmaceutical nanoparticles: Proof of concept. *Chem Eng Res Des.* 2009;87:543–9.
- [19] Marchisio DL. Large eddy simulation of mixing and reaction in a confined impinging jets reactor. *Comp Chem Eng.* 2009;33(2):408–20.
- [20] Icardi M, Gavi E, Marchisio DL, et al. Investigation of the flow field in a three-dimensional confined impinging jets reactor by means of microPIV and DNS. *Chem Eng J.* 2011;166(1):294–305.
- [21] Lince F, Marchisio DL, Barresi AA. A comparative study for nanoparticle production with passive mixers via solvent-displacement: Use of CFD models for optimization and design. *Chem Eng Process.* 2011;50:356-68.
- [22] Valente I, Celasco E, Marchisio DL, et al. Nanoprecipitation in confined impinging jet mixers: Production, characterization and scale-up of pegylated nanospheres and nanocapsules for pharmaceutical use. *Chem Eng Sci.* 2012;77:217-27.

[23] Lince F, Bolognesi S, Marchisio DL, et al. Preparation of poly(MePEGCA-co-HDCA) nanoparticles with confined impinging jets reactor: Experimental and modeling study. *J Pharm Sci.* 2011;100:2391-405.

[24] Han J, Zhu Z, Qian H, et al. A simple confined impingement jets mixer for flash nanoprecipitation. *J Pharm Sci.* 2012;101:4018-23.

[25] Zelenková T, Fissore D, Marchisio DL, et al. Size control in production and freeze-drying of poly- $\epsilon$ -caprolactone nanoparticles. *J Pharm Sci.* 2014;103:1839-50.

[26] Barresi AA, Vanni M, Fissore D, et al. Synthesis and preservation of polymer nanoparticles for pharmaceutical applications. In: Thakur VK, Thakur MK, editors. *Handbook of polymers for pharmaceutical technologies: Processing and applications, Volume 2.* Hoboken, NJ, USA: John Wiley & Sons Inc; 2015. pp. 229-280.

[27] Winzenburg G, Schmidt C, Fuchs S, et al. Biodegradable polymers and their potential use in parenteral veterinary drug delivery systems. *Adv Drug Deliver Rev.* 2004;56:1453–66.

[28] Eliaz RE, Kost J. Characterization of a polymeric PLGA-injectable implant delivery system for the controlled release of proteins. *J Biomed Mater Res.* 2000;50:388-96.

[29] Tang ZG, Rhodes NP, Hunt JA. Control of the domain microstructures of PLGA and PCL binary systems: Importance of morphology in controlled drug release. *Chem Eng Res Des.* 2007;85:1044–50.

[30] United States Pharmacopoeia. Florfenicol. United States Pharmacopoeial Convention, Rockville, MD; 2007.

[31] Song M, Li Y, Ning A, et al. Silica nanoparticles as a carrier in the controlled release of florfenicol. *J Drug Deliv Sci Tec.* 2010;20:349-52.

[32] Kou X, Li Q, Lei J, et al. Preparation of molecularly imprinted nanospheres by premix membrane emulsification technique. *J Membrane Sci.* 2012;417-418:87–95.

[33] Pinto RA, Torres PM, Luengo JE, et al. Development and characterization of PLGA nanoparticles loaded with florfenicol. *Lat Am J Pharm.* 2014;33:1139-43

[34] Wang T, Chen X, Lu M, et al. Preparation, characterisation and antibacterial activity of a florfenicol-loaded solid lipid nanoparticle suspension. *IET Nanobiotechnol.* 2015;9:355-361.

[35] Di Pasquale N, Marchisio DL, Barresi AA. Model validation for precipitation in solvent-displacement processes. *Chem Eng Sci.* 2012;84:671-83.

[36] Maia JL, Santana MHA, Ré MI. The effect of some processing conditions on the characteristics of biodegradable microspheres obtained by an emulsion solvent evaporation process. *Braz J Chem Eng.* 2004;21:1–12.

[37] Ye M, Kim S, Park K. Issues in long-term protein delivery using biodegradable microparticles. *J Control Release.* 2010;146:241–60.

[38] Turino LN, Mariano RN, Boimvaser S, et al. In situ-formed microparticles of PLGA from O/W emulsions stabilized with PVA: encapsulation and controlled release of progesterone. *J Pharm Innov.* 2014;9:132-40.

[39] Aubry J, Ganachaud F, Addad JPC, et al. Nanoprecipitation of polymethylmethacrylate by solvent shifting: 1. Boundaries. *Langmuir.* 2009;25:1970–9.

[40] Thakur VK, Kumari M. *Handbook of Polymers for Pharmaceutical Technologies, Structure and Chemistry.* Hoboken, NJ, USA: John Wiley & Sons Inc.; 2015.

[41] Alshamsan A. Nanoprecipitation is more efficient than emulsion solvent evaporation method to encapsulate cucurbitacin I in PLGA nanoparticles. *Saudi Pharm J.* 2014;22:219-22.

[42] Xie H, Smith JW. Fabrication of PLGA nanoparticles with a fluidic nanoprecipitation system. *J Nanobiotechnology.* 2010;8:18. doi: 10.1186/1477-3155-8-18.

[43] Misra R, Acharya S, Dilnawaz F, et al. Sustained antibacterial activity of doxycycline-loaded poly(D,L-lactide-*co*-glycolide) and poly( $\epsilon$ -caprolactone) nanoparticles. *Nanomedicine-UK*. 2009;4:519-30.

[44] Müller RH, Mäder K, Gohla S. Solid lipid nanoparticles (SLN) for controlled drug delivery – a review of the state of the art. *Eur J Pharm Biopharm*. 2000;50:161-77.

[45] Müller RH. Zetapotential und Partikelladung in der Laborpraxis. Einführung in die Theorie, Praktische Meßdurchführung, Dateninterpretation [Zeta potential and particle loading in laboratory practice. Introduction to theory, practical measurement execution, data interpretation], Wissenschaftliche Verlagsgesellschaft, Stuttgart; 1996.

[46] Corrigan OI, Li X. Quantifying drug release from PLGA nanoparticles. *Eur J Pharm Sci*. 2009;37:477-85.

[47] Lince F, Bolognesi S, Stella B, et al. Preparation of polymer nanoparticles loaded with doxorubicin for controlled drug delivery. *Chem Eng Res Des*. 2011;89:2410-9.

[48] Zili Z, Sfar S, Fessi H. Preparation and characterization of poly- $\epsilon$ -caprolactone nanoparticles containing griseofulvin. *Int J Pharm*. 2005;294:261–7.

[49] Barichello JM, Morishita M, Takayama K, et al. Encapsulation of hydrophilic and lipophilic drugs in PLGA nanoparticles by the nanoprecipitation method. *Drug Dev Ind Pharm*. 1999;25:471–6.

[50] Zakeri-Milani P, Badir Delf Loveymi BD, Jelvehgari M, et al. The characteristics and improved intestinal permeability of vancomycin PLGA-nanoparticles as colloidal drug delivery system. *Colloid Surface B*. 2013;103:174–81.

Table 1. Summary of preparation conditions and evaluated characteristics of nanoparticles

Operating parameter	Unloaded nanoparticles	Loaded nanoparticles 1	Loaded nanoparticles 2
Polymer type	PCL; PLGA	PCL; PLGA	PCL; PLGA
Solvent	Acetone	Acetone	Acetone
Anti-solvent	Water	Water	Water
Initial polymer concentration (mg/mL in acetone)	2.5; 6; 10	6	6
Flow rate (mL/min)	40; 80; 120	40; 80; 120	80
Anti-solvent-to-solvent flow rate ratio	1	1	1
Drug	-	Florfenicol	Florfenicol
Initial drug concentration (mg/mL in acetone)	-	0.5; 1; 2; 5	0.5; 1; 2; 5
Evaluated characteristics	Mean particle size, particle size distribution, surface zeta potential	Mean particle size, particle size distribution, surface zeta potential	Entrapment and encapsulation efficiency of drug by nanoparticles

Table 2. Mean particle size and zeta potential of nanoparticles obtained with 6 mg/mL of PCL under different flow rates (FR) and initial florfenicol concentrations.

	Florfenicol initial concentration (mg/mL in acetone)				
	0	0.5	1	2	5
FR (mL/min)	Size distribution (mean (SD), n = 3), nm				
40	280.0 (14.0)*,**	293.8 (4.9)*	282.7 (7.5)*,**	269.7 (9.0)**	284.8 (7.5)*,**
80	270.9 (24.6)*	286.5 (12.6)*	278.6 (3.0)*	264.3 (21.3)*	265.9 (9.9)*
120	265.8 (6.6)*	275.9 (5.4)*	263.7 (2.8)*	240.3 (15.3)*	275.0 (6.3)*
FR (mL/min)	Zeta potential (mean (SD), n = 3), mV				
40	-22.1 (0.5)	-21.2 (4.0)	-23.3 (0.9)	-20.7 (1.0)	-19.1 (2.2)
80	-22.1 (1.1)	-21.1 (0.9)	-26.3 (3.5)	-20.2 (2.0)	-18.5 (4.4)
120	-20.6 (1.2)	-20.9 (0.8)	-23.3 (1.3)	-20.1 (1.5)	-18.2 (2.3)

\*,\*\*Means statistically equals between columns ( $p > .05$ ).

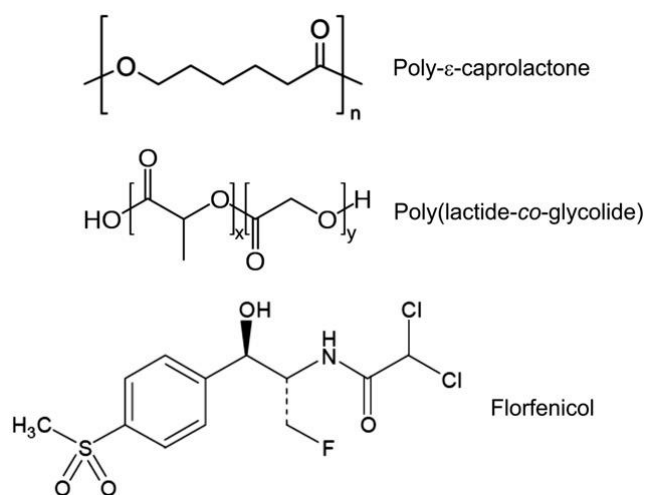
Table 3. Mean particle size and zeta potential of nanoparticles obtained with 6 mg/mL of PLGA under different flow rates (FR) and initial florfenicol concentrations.

	Florfenicol initial concentration (mg/mL in acetone)				
	0	0.5	1	2	5
FR (mL/min)	Size distribution (mean (SD), n = 3), nm				
40	101.8 (3.0)*	100.7 (4.6)*	93.6 (6.0)*,**	91.2 (4.8)**	101.9 (3.9)*
80	93.5 (4.7)*	95.4 (6.0)*	95.4 (11.4)*	97.4 (16.6)*	95.4 (2.9)*
120	81.7 (0.6)*	78.1 (4.2)*	80.0 (5.2)*	80.5 (9.2)*	78.1 (5.2)*
FR (mL/min)	Zeta potential (mean (SD), n = 3), mV				
40	-37.3 (1.4)	-41.4 (5.2)	-31.7 (2.5)	-37.5 (2.5)	-37.6 (3.2)
80	-38.1 (1.6)	-32.4 (6.4)	-30.8 (3.8)	-35.4 (3.7)	-36.1 (10.0)
120	-34.4 (3.1)	-37.5 (4.2)	-36.8 (1.5)	-37.0 (3.0)	-38.8 (5.2)

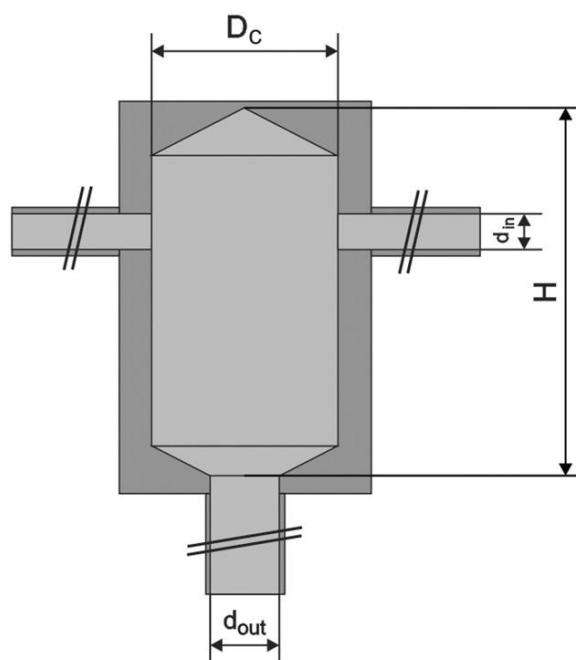
\*\*\* Means statistically equals between columns ( $p > .05$ ).

Table 4. Mean (and standard deviation) florfenicol entrapment (En, % w/w) of loaded nanoparticles based on 6 mg/mL of polymer and flow rate of 80 mL/min.

Polymer	Florfenicol initial concentration (mg/mL in acetone)			
	0.5	1	2	5
PCL	0	0	1.54 (0.14)	10.12 (0.37)
PLGA	0.76 (0.10)	2.21 (0.19)	5.39 (0.27)	12.93 (0.48)



**Fig. 1** Chemical structures of considered polymers and drug



**Fig. 2** Scheme of the confined impinging jet mixer used.  $D_c=4.8$  mm,  $d_{in}=1$  mm,  $d_{out}=2$  mm;  $H$  is approximately equal to  $2D_c$

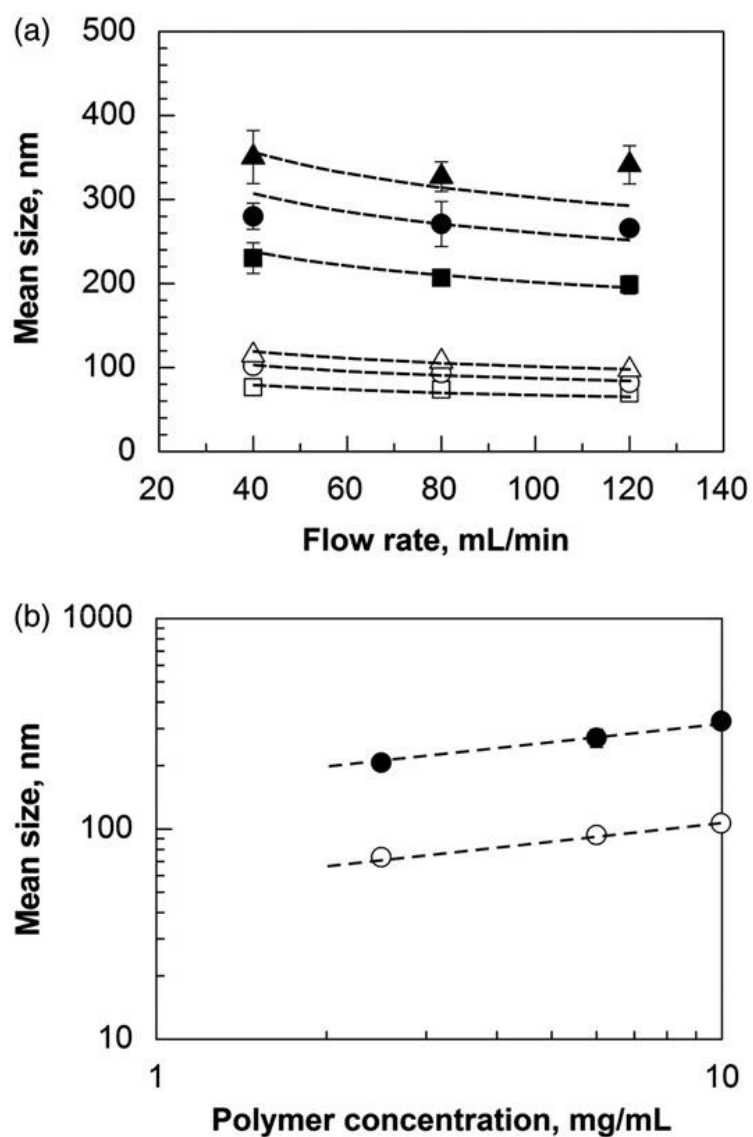


**Fig. 3** Mean size of PCL (filled symbols) and PLGA (empty symbols) nanoparticles obtained under different flow rates (a) for (■,□) 2.5, (●,○) 6 and (▲,△) 10 mg/mL of polymer, and under different polymer concentrations (b) at flow rate 80 mL/min. The trend lines were calculated using Eq. (3), with  $\alpha=0.29$  and  $\beta=-0.18$ ; error bars in Fig. 3b are smaller than symbols.

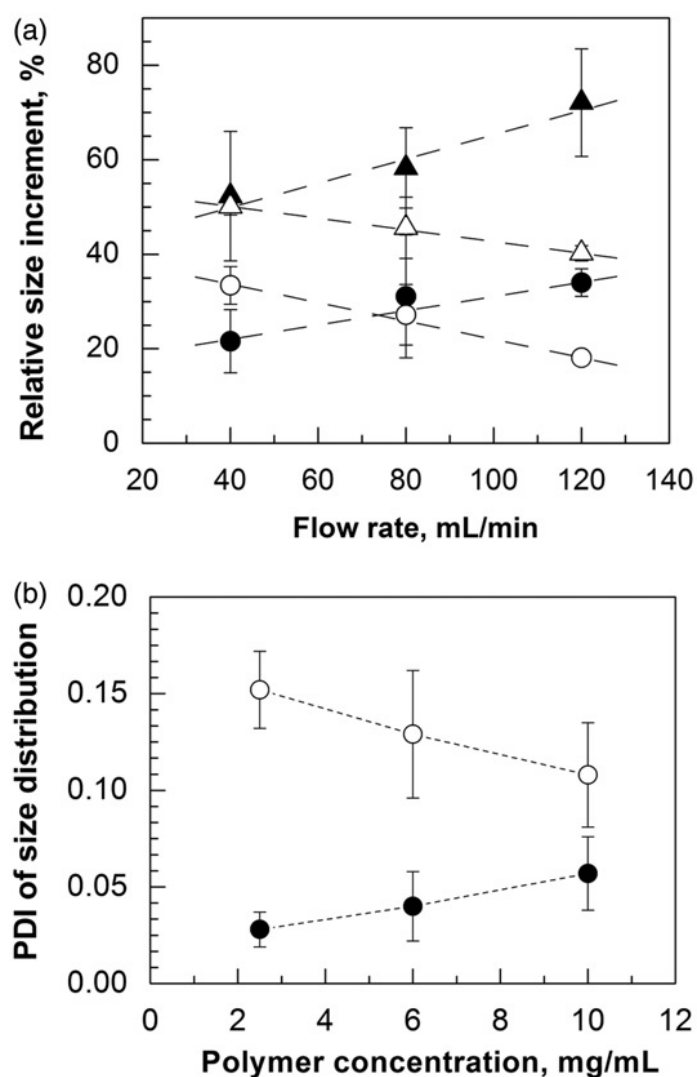


**Fig. 4** Relative mean size increment (a) under different flow rates for (●,○) 6 and (▲,△) 10 mg/mL of polymer, and polydispersity index of size distribution (b) under different polymer concentrations (flow rate 80 mL/min) for nanoparticles obtained with PCL (filled symbols) and PLGA (empty symbols).

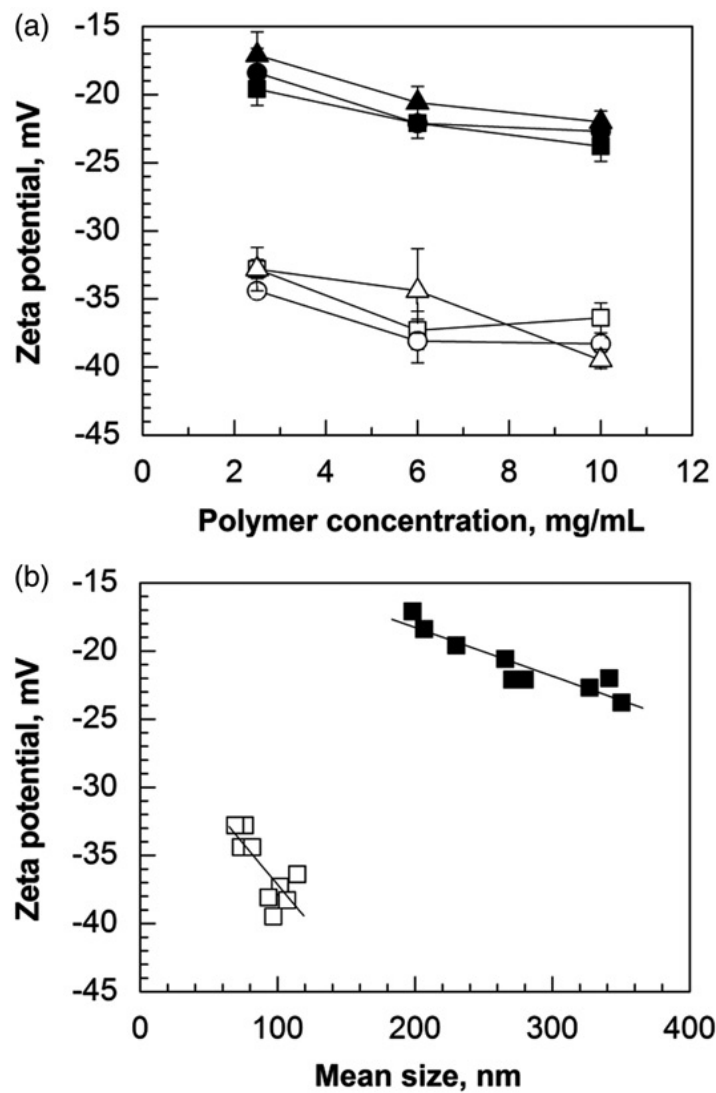


**Fig. 5** (a) Zeta potential of nanoparticles obtained with different concentrations of PCL (filled symbols) and PLGA (empty symbols) at flow rates of (▲,△) 40, (●,○) 80 and (■,□) 120 mL/min. (b) Relationship between the mean particle size and zeta potential of nanoparticles formed by (■) PCL and (□) PLGA.